JPE 18-5-19

https://doi.org/10.6113/JPE.2018.18.5.1501
ISSN(Print): 1598-2092 / ISSN(Online): 2093-4718

Three-Phase Three-Switch Buck-Type Rectifier Based on Current Source Converter for 5MW PMSG Wind Turbine Systems

Beomseok Chae*, Yongsug Suh†, and Tahyun Kang**

†,*Department of Electrical Engineering, Chonbuk National University, Jeonju, Korea
**R&D Center, Milimsyscon, Seoungnam, Korea

Abstract

This paper proposes a three-phase three-switch buck-type converter as the MSC of a wind turbine system. Owing to a novel switching modulation scheme that can eliminate the unwanted diode rectifier mode switching state, the proposed system exhibits a satisfying ac voltage and current waveform quality and torque ripple up to the level of a typical current source rectifier even under a wide power factor operating range. The proposed system has been verified through simulations and HILS tests on a PMSG wind turbine model of 5MW/4160V. The proposed converter has been shown to provide a stator current THD of 3.9% and a torque ripple of 1% under the rated power condition. In addition to the inherent advantage of the reduced switch count of three-phase three-switch buck-type converters, the proposed switching modulation technique can make this converter a viable solution for the MSC placed inside of a nacelle, which is under severe volume, weight and mechanical vibration design limits.

Key words: Carrier based PWM, Current source rectifier, Three-phase three-switch buck-type rectifier

I. INTRODUCTION

The demand for sustainable and renewable energy has been increased remarkably due to the energy crisis and environmental concerns. Among renewable energy sources, wind energy capacity has been increasing rapidly over the last decade. According to recent trends, the power generation capability of an individual wind turbine is moving from the kW class to MW class to reduce the cost of an installation in terms of generated energy. When the power capacity of an individual wind turbine system increases, in order to reduce the current level, a Medium Voltage (MV) system can be adopted for the power converter and generator of the wind turbine [1]-[3]. MV converter have become preferable when compared to the parallel connection of Low Voltage (LV) converters due to their lower component count, higher efficiency and simpler power stage design when used in the power converters of wind turbines [4].

Various topologies and control methods have been developed for wind turbine systems. Current source type converters have been regarded as one of the more interesting circuit topologies in the motor drives of MV class converter due to their inherent short circuit protection capability and low dv/dt characteristic of ac line voltage in long range cable connections [5]. Some work has been done for current source rectifier-based wind turbine systems [6], [7]. Among the many current source type converters, the three-phase three-switch buck-type converter is a candidate topology for the Machine Side Converters (MSCs) of wind turbine systems. This three-phase three-switch buck-type converter consists of four diodes and only one active switch per phase. It has a total of twelve diodes and three active switches in the MSC of the three-phase switch resulting in a reduced component count when compared to conventional current source converters. This reduced switch count makes the three-phase three-switch buck-type converter an attractive solution for the MSCs that are usually mounted within nacelle of wind turbines since they are subject to relatively critical design limitations in terms of volume, weight and mechanical vibration [8].

Manuscript received Mar. 15, 2018; accepted May 31, 2018
Recommended for publication by Associate Editor Dong-Myung Lee.
†Corresponding Author: ysuh@jbnu.ac.kr
Tel: +82-63-270-2389, Fax: +82-63-270-2394, Chonbuk Nat'l Univ.
*Dept. of Electrical Engineering, Chonbuk National University, Korea
**R&D center, Milimsyscon, Korea

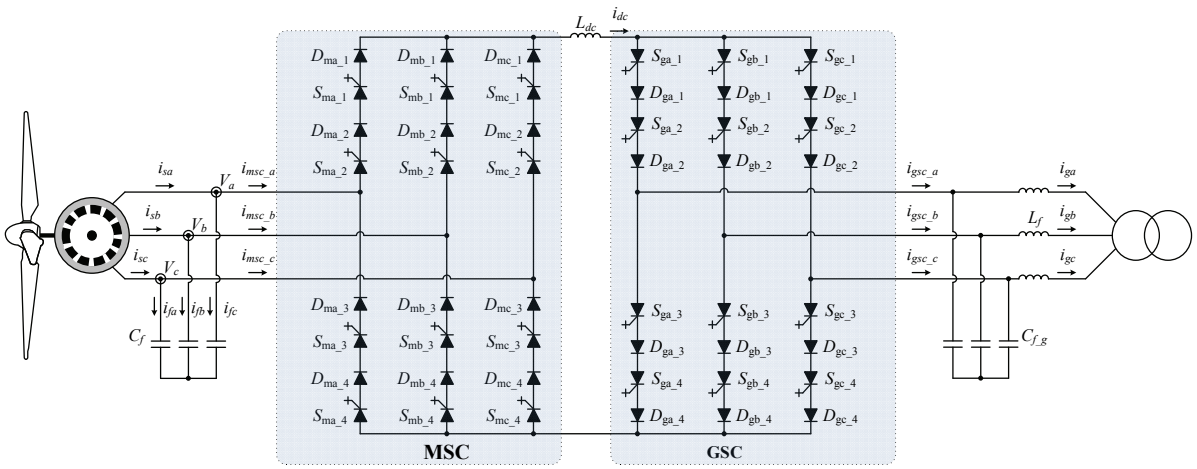

Fig. 1. Back-to-back type current source rectifier-based converters for 5MW PMSG MV wind turbines.

Despite the advantage of a reduced number of switches, the three-phase three-switch buck-type converter has an inherent fatal problem in terms of a limited power factor operating range due to the structure of the switch cell. Therefore, when the ac machine side voltage and current require a power factor angle beyond the possible operating range of the converter, the switching modulation becomes disrupted leading to severe harmonic distortions of the ac voltage and current. This property of a limited power factor operating range prohibits three-phase three-switch buck-type converters from being successfully applied to the MSCs of wind turbine systems. This is because the Permanent Magnet Synchronous Generators (PMSGs) or Doubly-Fed Induction Generators (DFIGs) employed in typical wind turbine systems demand some reactive power to sustain the magnetizing current of machines. There has been some previous research trying to increase the power factor operating range by various switching modulation techniques for three-phase three-switch buck-type converters [9]-[11]. However, none of them have paid enough attention to the practical switching modulation scheme to satisfy the unique operating requirements of wind turbine systems in the MW range.

This paper investigates the application of three-phase three-switch rectifiers as the MSC in a wind turbine system. By employing a novel switching modulation scheme, the proposed system can be nicely fit into wind turbine systems requiring a wide power factor operating range in the ac machine side. This novel switching modulation scheme avoids the unwanted diode rectifier switching state by providing an accurate switching path for the ac input current with respect to the reference command of the ac input current under a wide power factor operating range. The performance of the proposed system is compared with that of the conventional current source type rectifier in the MSC of a wind turbine system. A wind turbine of the 5MW/4.16 kV Permanent Magnet Synchronous Generator (PMSG) type is chosen as a common platform for the comparison. In other words, a back-to-b ack type current source rectifier-based converter, which is regarded as the most popular type of current source topology choice in the power range of 5MW, and the proposed back-to-back three-phase three-switch rectifier topology are analyzed and compared. The performances of the two different types of converter systems are studied with respect to the PMSG performance factor of stator currents and torque ripples.

The main objective of this paper is to show that the proposed three-phase three-switch buck-type rectifier can work well as the MSC of a wind turbine system at a similar performance level as a conventional current source rectifier. This paper is structured in six main sections as follows. Section II provides the power semiconductor devices and system specification under comparison of a 5MW PMSG Wind Turbine System (WTS). In Section III, the operating principles of a three-phase three-switch buck-type rectifier are described. Section IV explains a novel switching modulation technique for the three-phase three-switch buck-type rectifier. Section V presents some simulation and HILS test results of the proposed system in a 5MW PMSG WTS. Finally, some conclusions are given in Section VI.

II. Current Source Rectifier and Three-Phase Three-Switch Buck-Type Rectifier for Wind Turbine Systems

A. Current Source Rectifier

Fig. 1 shows a schematic of a two-level current source rectifier with a series connection of two IGCTs, i.e. ns=2. The series connection of two devices is required to achieve an ac line input of 4.16kV. Each leg of the current source converters consists of four switches (Sm_x, Sg_x), and four reverse blocking diodes (Dm_x, Dg_x) [5]. The DC-Link current Idc should be continuous. Therefore, the zero switching state of the current source rectifier is equivalent to

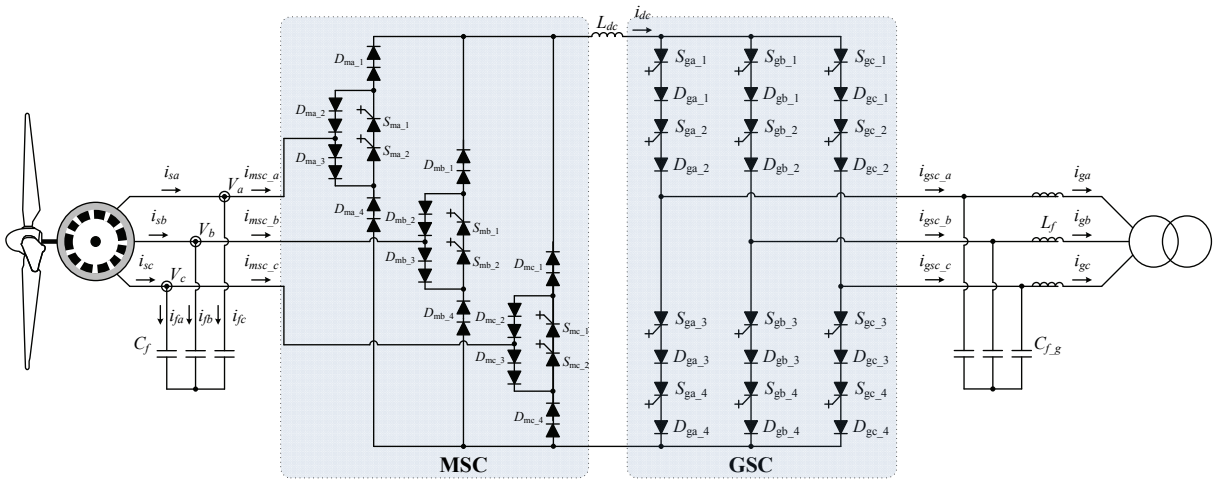

Fig. 2. Newly proposed structure for the back-to-back type three-phase three-switch buck-type converters of 5MW PMSG MV wind turbines.

shorting one of the three phase legs in the converter. In general, this placement of zero state vector complicates the control of the current source rectifier when compared to the voltage source rectifier [12].

B. Three-Phase Three-switch Buck-Type Rectifier

In this paper, a new concept for a wind turbine converter is proposed. Fig. 2 shows a schematic of a three-phase three-switch buck-type rectifier with a series connection of two IGCTs, i.e. ns=2. The series connection of the two devices is required to meet an ac line input of 4.16kV. Each of the legs of the three-phase three-switch buck-type rectifier in the Machine Side Converter (MSC) consists of four reverse blocking diodes (Dm_x) and two IGCT switchers (Sm_x) per leg. As a result, the proposed MSC when compared to the conventional MSC in Fig. 1 has a reduced device count of the active switch by half. The Grid Side Converter (GSC) is based on a conventional current source inverter. Each of the legs of the GSC consists of four switches (Sg_x), and four reverse blocking diodes (Dg_x). The conventional current source inverter is adopted in the GSC in order to meet the grid code of wide power factor operation [14].

C. Power Semiconductor Devices

In this paper, the current source rectifier and three-phase three-switch buck-type rectifier employ the same switching devices of a press-pack IGCT (ABB 5SHY 42L6500) and a press-pack FRD (ABB 5SDF 10H6004) for the sake of a consistent and fair comparison of the two topologies. The main characteristics of the employed power semiconductor devices are summarized in Table I [5].

D. System Specifications

In this paper, the current source rectifier and three-phase three-switch buck-type rectifier employ the same switching devices of a press-pack IGCT (ABB 5SHY 42L6500) and a press-pack FRD (ABB 5SDF 10H6004) for the sake of a consistent and fair comparison of the two topologies. The main characteristics of employed power semiconductor devices are summarized in Table I [5].

TABLE I
DEVICE PARAMETERS OF POWER SEMICONDUCTOR [5]

Device	Press-pack IGCT	Press-pack Diode
Manufacture	ABB	ABB
Code	5SHY 42L6500	5SDF 10H6004
Blocking Voltage	6.5 kV	6.0 kV
$I_{TGQM}/I_{F(AV)M}$	3.8 kA	1.1 kA

III. CURRENT COMMUTATION AND SWITCHING STATES OF A THREE-PHASE THREE-SWITCH BUCK-TYPE RECTIFIER

In the basic operation of the circuit, the three switches can exercise complete control over the conduction of all the respective branches as illustrated in Fig. 3. There are two states of current commutation, i.e. the two-switch turn-on mode and the diode rectifier mode (all of the switches are turn-on) [9]. The two-switch turn-on mode implies the case when two out of three active switches are turned on. During this mode the effective current path is determined by the polarity of the input capacitor line voltages. The phase with the larger supply voltage is connected to the positive bar and the phase with smaller supply voltage is connected to the negative bar of the DC-Link as shown Fig. 4. The diode rectifier mode represents the case when all of the switches are turned on. The input phase of the largest voltage amplitude is connected to the positive bar and the input phase of the smallest voltage amplitude is connected to the negative bar of the DC-Link as illustrated in Fig. 5. The converter input currents under each of the switching states are presented in

TABLE II
PARAMETERS OF A 5MW PMSG WIND TURBINE SYSTEM

Parameter	Symbol	Value	Per unit
Rated power	P_m	5 MW	1.0
Rated wind speed	V_w	11.8 m/s	-
Rated stator voltage	V_m	4.16 kV	1.0
Rated q-axis current	I_{qs}	1,007 A	1.0
Rated stator frequency	f_{pm}	29.1 Hz	1.0
Rated rotor speed	ω_r	14.8 rpm	-
Rated rotor flux linkage	λ	18.0926 Wb	-
Rated mechanical torque	T_m	3.226 MN.m	-
Pole pairs	Z_p	118	-
Inertia	J	2.5e5 kg.m^2	-
Stator resistance	R_s	80 mΩ	-
d-axis magnetizing inductance	L_{md}	5.5963 mH	-
q-axis magnetizing inductance	L_{mq}	5.5963 mH	-
PWM carrier frequency	f_{SW}	2,000 Hz	-
Grid frequency	f_{grid}	60 Hz	1.0
Grid side input voltage	V_{LL}	4.16 kV	1.0
Grid side input current	I_{AC_input}	708 A	1.0
Grid side filter inductance	L_f	0.98 mH	0.11
AC filter capacitance	C_{f_g}	0.26 mF	0.34
DC-Link current	I_{DC}	997 A	-
DC-Link inductance	L_{DC}	8.3 mH	-

WTS. Finally, some conclusions are given in Section VI.

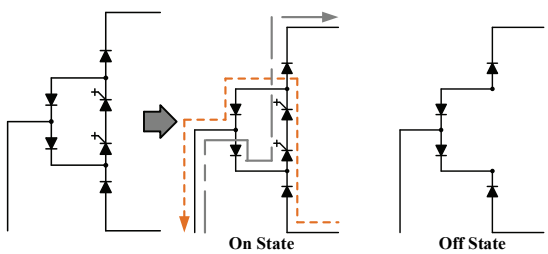

Fig. 3. Switch states and current paths of the on/off switching modes in a simplified schematic for a three-phase three-switch buck-type rectifier.

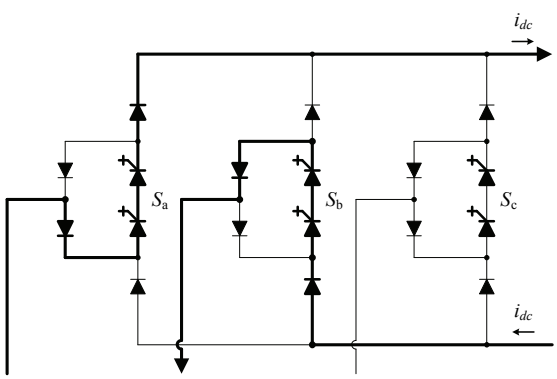

Fig. 4. Switch states and current paths in a simplified schematic of a three-phase three-switch buck-type rectifier under the active switching mode and V_a>V_b.

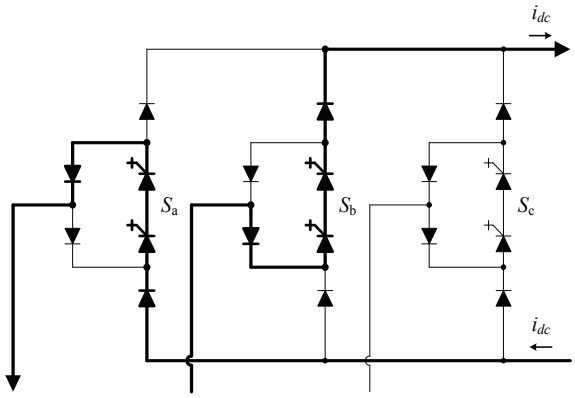

Fig. 5. Switch states and current paths in a simplified schematic of a three-phase three-switch buck-type rectifier under the diode rectifier mode (all of the switches are turn-on) and V_b>V_c>V_a.

TABLE III
ACTIVE SWITCHING AND ZERO SWITCHING STATE FOR A THREE-PHASE THREE-SWITCH BUCK-TYPE RECTIFIER

Switching State	I_{msc_a}	I_{msc_b}	I_{msc_c}	Zero/Active
(000) (100), (010), (001)	0	0	0	Zero Switching
(110)	$\pm I_{dc}$	$\pm I_{dc}$	0	Active Switching
(011)	0	$\pm I_{dc}$	$\mp I_{dc}$	
(101)	$\pm I_{dc}$	0	$\mp I_{dc}$	
(111)	$\pm I_{dc}$	$\pm I_{dc}$	$\pm I_{dc}$	

TABLE IV
SECTORS OF THE CONVERTER INPUT CURRENT

Sector	Converter input current	a-phase current angle (degree)
S1	I_a>I_c>I_b	30~90
S2	I_a>I_b>I_c	90~150
S3	I_b>I_a>I_c	150~210
S4	I_b>I_c>I_a	210~270
S5	I_c>I_b>I_a	270~330
S6	I_c>I_a>I_b	330~30

Table III. When all of the IGCT switches are conducting, i.e. the diode rectifier mode, the phase currents and switching states depend on the actual polarity of the capacitor line voltages. In Table IV, the period of the a-phase current is divided into six time intervals according to the relative magnitude of the three-phase converter input currents. The sector name and its corresponding current angles defined in Table IV are used throughout this paper, unless stated otherwise.

IV. Modulation Strategy of Three-Phase Three-Switch Buck-Type Rectifiers

A. General Modulation Strategy Under the Unity Power Factor Condition at the Converter AC Input Side

One leg of a three-phase three-switch buck-type rectifier is driven by only one switch. This switch drives both the positive current and negative current at the ac side. As a result, a rectified reference current with a positive amplitude is compared with a unipolar triangular carrier at the switching frequency under pulse width modulator, which is contrary to the case of a typical voltage source converter. This PWM action is explained in Fig. 6 for the case of Sector 1 (I_a>I_c>I_b). If the *a*-phase switch (S_a) is turned on, the *a*-phase converter input current (I_a) has a positive value under the condition of V_a>V_c>V_b. In the same manner, I_b has a negative value when the *b*-phase switch (S_b) is turned on under the same condition of V_a>V_c>V_b. The *c*-phase is dependent on S_a and S_b. The *c*-phase converter input current (I_c) has a negative value when S_a and S_c are turned on at the same time. Using the same reasoning, S_b and S_c are turned on, then the I_c becomes positive. When all of the switches are turned on, the diode rectifier mode, I_c is zero because the *c*-phase voltage (V_c) takes the median value between V_a and V_b.

In a balanced 3-phase 3-wire system, the sum of the 3-phase current is always zero. i.e. I_a+I_b+I_c=0. As stated above, I_c is dependent on S_a and S_b. However, I_a and I_b are independent from the other phase switching condition when voltages are V_a>V_c>V_b and current is in-phase with the voltage at the converter ac input (I_a>I_c>I_b, Sector 1).

As a result, I_a and I_b are independently modulated according to the given reference signals as shown in Fig. 6. Meanwhile, I_c is naturally determined from the relationship of I_a+I_b+I_c=0.

In general, the switch of a particular phase leg turns on when the rectified reference current of the corresponding phase becomes larger than the triangular carrier waveform. However, the switch of a phase leg whose current amplitude takes a median value among three-phase currents is kept turned on, e.g. S_c in Sector 1, irrespective of the other two switches. Once the switch turns on, the sign of the converter input current flowing through that particular switch is determined by the sign of the line voltage at the input capacitor as illustrated in Fig. 7. The waveforms of Fig. 6 and 7 are drawn in the same time scale and incidence.

According to the PWM action described in Fig. 6 and 7, a total of three possible switching states can be generated in each sub-sector. Table V summarizes these three possible switching states and their corresponding current polarities under the particular operating conditions of Sector 1-1 (30°~60°) and Sector 1-2 (60°~90°). Each of the current sub-sectors has three switching states. These states consist of one zero switching and two active switching states. For example, Sector 1-1 (30°~60°) has the (001) state as zero switching, and the (011) and (111) states as active switching. The (111) switching state is called the diode rectifier mode. Under the in-phase condition, there is no problem modulating the converter input currents according to the given current reference signals. However, under the non-unity power factor condition at the converter ac input side, i.e. when the relative amplitudes of the current references are different from those of the converter ac input voltage, the modulation strategy described in Table V generates unwanted current flow paths under the diode rectifier mode. This problem is further explained in the next section.

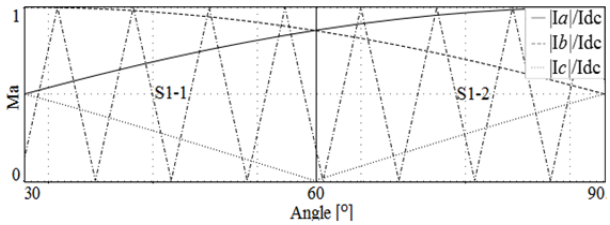

Fig. 6. Absolute modulation signal of the converter input currents and triangular carrier waveform under sector 1(S1), (I_a>I_c>I_b).

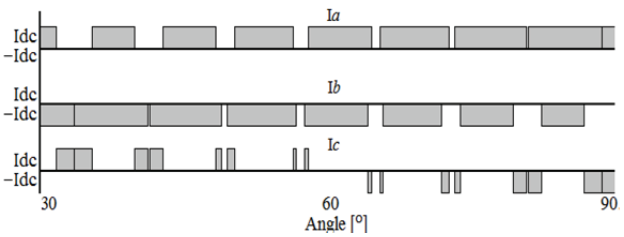

Fig. 7. Converter input currents of each phase under sector 1(S1), (I_a>I_c>I_b).

TABLE V
Active Switching and Zero Switching State at Sector *S1*

Sector *S1*-1 (30°~60°)				Sector *S1*-2 (60°~90°)			
Switching State	I_a	I_b	I_c	Switching State	I_a	I_b	I_c
(001)	0	0	0	(001)	0	0	0
(011)	0	$-I_{dc}$	I_{dc}	(101)	I_{dc}	0	$-I_{dc}$
(111)	I_{dc}	$-I_{dc}$	0	(111)	I_{dc}	$-I_{dc}$	0

B. Problem of the Diode Rectifier Mode Under the Non-Unity Power Factor Condition at the Converter AC Input Side

The input currents are dependent on the relative amplitude of the three phase capacitor voltages under the diode rectifier mode having the switching state of (111). The path of the current flowing changes when the sector of the input capacitor voltage is changed. In Sector 1-1, the *a*-phase current path is connected to the positive bar in the dc-side, the *b*-phase current path is connected to the negative bar in the dc-side, and the *c*-phase current path is connected to the

TABLE VI
PHASE CURRENT UNDER VARIABLE VOLTAGE CONDITIONS WITH THE CONVENTIONAL METHOD

Sector S1-1
$I_a>I_c>I_b$ ($|I_b|>|I_a|>|I_c|$)

	$V_c>V_a>V_b$ $0^\circ <$ leading angle $< 30^\circ$			$V_a>V_c>V_b$ In-phase			$V_a>V_c>V_b$ $0^\circ <$ leading angle $< 30^\circ$		
	I_a	I_b	I_c	I_a	I_b	I_c	I_a	I_b	I_c
(110)	I_{dc}	$-I_{dc}$	0	I_{dc}	$-I_{dc}$	0	I_{dc}	$-I_{dc}$	0
(011)	0	$-I_{dc}$	I_{dc}	0	$-I_{dc}$	I_{dc}	0	$-I_{dc}$	I_{dc}
(111)	0	$-I_{dc}$	I_{dc}	I_{dc}	$-I_{dc}$	0	I_{dc}	$-I_{dc}$	0

Sector S1-2
$I_a>I_c>I_b$ ($|I_a|>|I_b|>|I_c|$)

	$V_c>V_a>V_b$ $0^\circ <$ leading angle $< 30^\circ$			$V_a>V_c>V_b$ In-phase			$V_a>V_c>V_b$ $0^\circ <$ leading angle $< 30^\circ$		
	I_a	I_b	I_c	I_a	I_b	I_c	I_a	I_b	I_c
(110)	I_{dc}	$-I_{dc}$	0	I_{dc}	$-I_{dc}$	0	I_{dc}	$-I_{dc}$	0
(101)	I_{dc}	0	$-I_{dc}$	I_{dc}	0	$-I_{dc}$	I_{dc}	0	$-I_{dc}$
(111)	I_{dc}	$-I_{dc}$	0	I_{dc}	$-I_{dc}$	0	I_{dc}	0	$-I_{dc}$

TABLE VII
PHASE CURRENT UNDER VARIABLE VOLTAGE CONDITIONS WITH THE PROPOSED METHOD

Sector S1-1
$I_a>I_c>I_b$ ($|I_b|>|I_a|>|I_c|$)

	$V_c>V_a>V_b$ $0^\circ <$ leading angle $< 30^\circ$			$V_a>V_c>V_b$ In-phase			$V_a>V_c>V_b$ $0^\circ <$ leading angle $< 30^\circ$		
	I_a	I_b	I_c	I_a	I_b	I_c	I_a	I_b	I_c
(110)	I_{dc}	$-I_{dc}$	0	I_{dc}	$-I_{dc}$	0	I_{dc}	$-I_{dc}$	0
(011)	0	$-I_{dc}$	I_{dc}	0	$-I_{dc}$	I_{dc}	0	$-I_{dc}$	I_{dc}
(110)	I_{dc}	$-I_{dc}$	0	I_{dc}	$-I_{dc}$	0	I_{dc}	$-I_{dc}$	0

Sector S1-2
$I_a>I_c>I_b$ ($|I_a|>|I_b|>|I_c|$)

	$V_c>V_a>V_b$ $0^\circ <$ leading angle $< 30^\circ$			$V_a>V_c>V_b$ In-phase			$V_a>V_c>V_b$ $0^\circ <$ leading angle $< 30^\circ$		
	I_a	I_b	I_c	I_a	I_b	I_c	I_a	I_b	I_c
(110)	I_{dc}	$-I_{dc}$	0	I_{dc}	$-I_{dc}$	0	I_{dc}	$-I_{dc}$	0
(101)	I_{dc}	0	$-I_{dc}$	I_{dc}	0	$-I_{dc}$	I_{dc}	0	$-I_{dc}$
(110)	I_{dc}	$-I_{dc}$	0	I_{dc}	$-I_{dc}$	0	I_{dc}	$-I_{dc}$	0

positive bar. In Table VI, these values of the phase currents are shown under the column of the in-phase condition. When the voltage condition is changed from the in-phase to the out-of-phase condition, the positive and negative DC-Links are connected to different ac phases when compared to the in-phase condition. For example, in Sector 1-1 under the leading angle condition between 0° and 30°, the values of the phase currents during the diode rectifier mode having the switching state of (111) are different from those under the in-phase condition. These different phase current values result in a failure of the pulse width modulation where the localized average value of the modulated current waveform is supposed to follow the reference signal of the phase current. In a similar manner, the values of the phase currents in Sector 1-2 become distorted under the lagging angle condition between 0° and 30° as shown in Table VI. Therefore, the transition of the voltage phase conditions may have a crucial impact on the path of the current flowing. This leads to a distortion of the converter input current when the converter input current and capacitor voltage have a phase angle difference [9].

C. Proposed Modulation Scheme Under the Non-Unity Power Factor Condition at the Converter AC Input Side

In this paper, an advanced modulation scheme and its simple digital implementation method for the back-to-back three-phase three-switch buck-type converters of Fig. 2 has been proposed. This newly proposed modulation scheme prevents failures of the pulse width modulation of the input phase current due to the diode rectifier mode having the switching state of (111) for the MSC in PMSG wind turbines. This is made possible by replacing the switching state of (111) with its equivalent active switching state, which generates the correct values of the phase currents depending on the operating sector. The selection of the switching combination in the improved modulation strategy is presented in Table VII. For example, in Sector 1-1 the diode rectifier mode is replaced by the switching state of (110). As a result, the values of the phase currents under the leading angle condition become equal to those of the in-phase condition. In the same manner, in Sector 1-2, the diode rectifier mode is also replaced by the switching state of (110). This replacement corrects the values of the phase currents under the lagging angle condition to match those of the in-phase condition. As a result, this replacement of the diode rectifier mode by the switching state of (110) in Sector 1 makes it possible that the current path is less affected by the transition of the voltage phase conditions [9]. The particular switching state in the substitution of the diode rectifier mode varies depending on the corresponding sector in Table IV.

In this paper, the advanced modulation scheme without the diode rectifier mode is newly implemented in Carrier Based PWM (CBPWM). The practical implementation of this CBPWM using digital logic gates is shown in Fig. 8. In this figure, the Switching Signal Generator Block is a typical sine-triangle modulator (①) in which a rectified sine modulating waveform of the positive value is compared with a unipolar triangular carrier waveform. In the Switching Signal Generator Block, there are three NXOR gates: ②-a, ②-b, and ②-c. Each of the NXOR gates only generates a high value when its corresponding phase current becomes a median phase, i.e. the amplitude of the corresponding phase current is the middle among three phase currents. For example, the output of ②-a becomes high when the reference

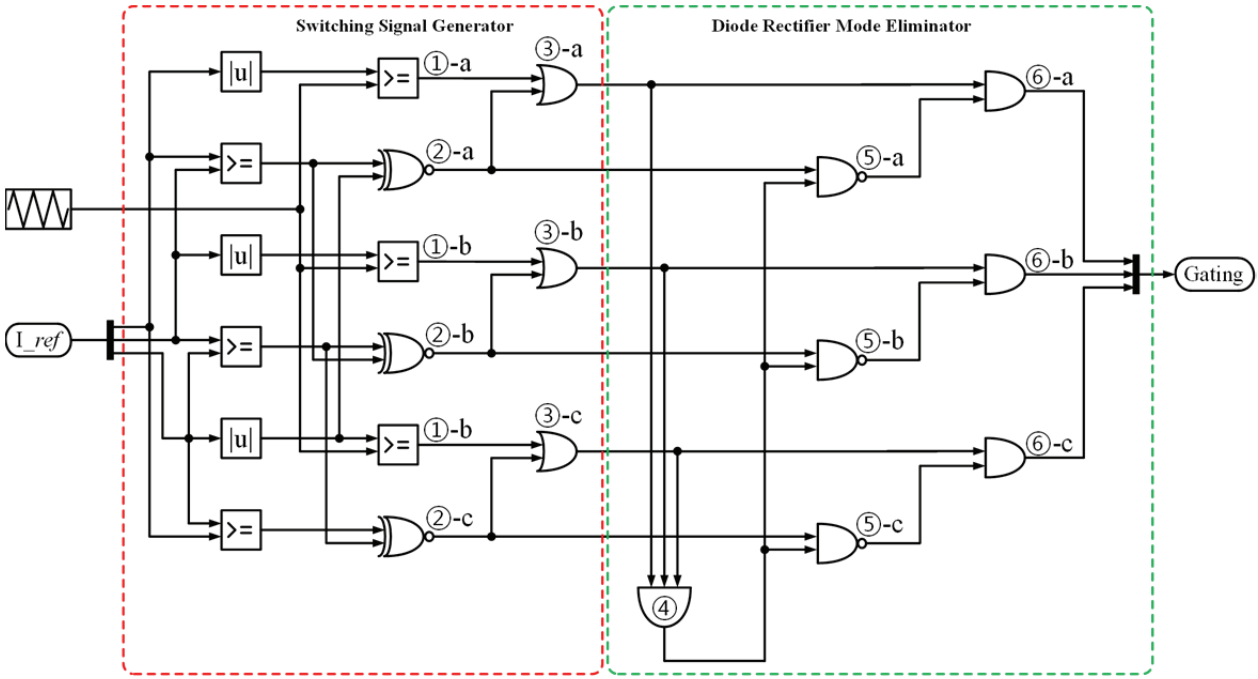

Fig. 8. Proposed modulation block of a three-phase three-switch buck-type rectifier.

signal of the *a*-phase converter input current becomes a median phase among the three phase currents.

The output signals of ①-a and ②-a are applied to the OR gate of ③-a. This is to ensure that, in addition to the action of the sine-triangle, the switch of the *a*-phase is turned on whenever the *a*-phase becomes a median phase. This is doen in order to provide a return path through the converter switch of the *a*-phase. In general, the OR gate of ③-a is indispensable for the switching modulation of current source type converters. Usually, voltage source type converters do not require this OR gate in PWM logic since each phase is modulated independently from the other remaining phases.

In Fig. 8, the Diode Rectifier Mode Eliminator Block implements the proposed modulation scheme. The output of the OR gate (③-a) is then masked by the AND gate of ⑥-a. This masking condition makes this modulation block different from state-of-the-arts solutions. The proposed masking condition is provided from the NAND gate of (⑤-a). This masking condition is triggered when the diode rectifier mode and the median phase condition are met at the same time. In other words, under the condition of the diode rectifier mode and a median phase, the turn-on signal for the switch of the corresponding phase is forced off, i.e. masking out. The diode rectifier mode of the switching state (111) is detected when the output of the AND gate (④) is high. Finally, the output of the AND gate of ⑥-a is applied to the *a*-phase switch of the converter. This final output represents the switching table as given in Table VII. The actions of the gates belonging to the *b*-phase and the *c*-phase are similar to those of the *a*-phase.

V. Simulation and Experiment Results

The current source rectifier based WTS of Fig. 1 and the three-phase three-switch buck-type rectifier based WTS of Fig. 2 have been simulated using PLECS. The two different topologies are verified through the real-time Hardware In the Loop (HIL) system of the RT-Box. The two different topologies are compared with respect to two major performance factors: the Total Harmonic Distortion (THD) of the PMSG stator current and the torque ripple under the rated power condition.

The simulation is made based on the operating condition specified in Table II. The two different topologies considered in this paper adopt the same overall control scheme for the MSC and GSC. Fig. 9 shows an overall control block diagram of a 5MW PMSG wind turbine system [13]. The employed real-time HIL system setup is illustrated in Fig. 10. Figures 11 through 15 present simulation waveforms of the current source rectifier based the WTS, particularly for the MSC. In this paper, both converters operate under the rectifier mode, i.e. power flows from the PMSG to the DC-Link. The capacitor voltages are described in Fig. 11. In Fig. 12, along with the capacitor voltage of the *a*-phase, the ripple currents of the capacitor filter are also shown. The typical chopped converter input currents of the MSC are described in Fig. 13 along with a filtered sinusoidal waveform of the stator current of the *a*-phase. The stator currents for all three of the phases and their frequency spectrums are given in Fig. 14. As expected, the chopped converter input currents are effectively filtered out by the input capacitor filter network between the machine and the current source rectifier of the MSC. Finally, the electromagnetic torque generated by

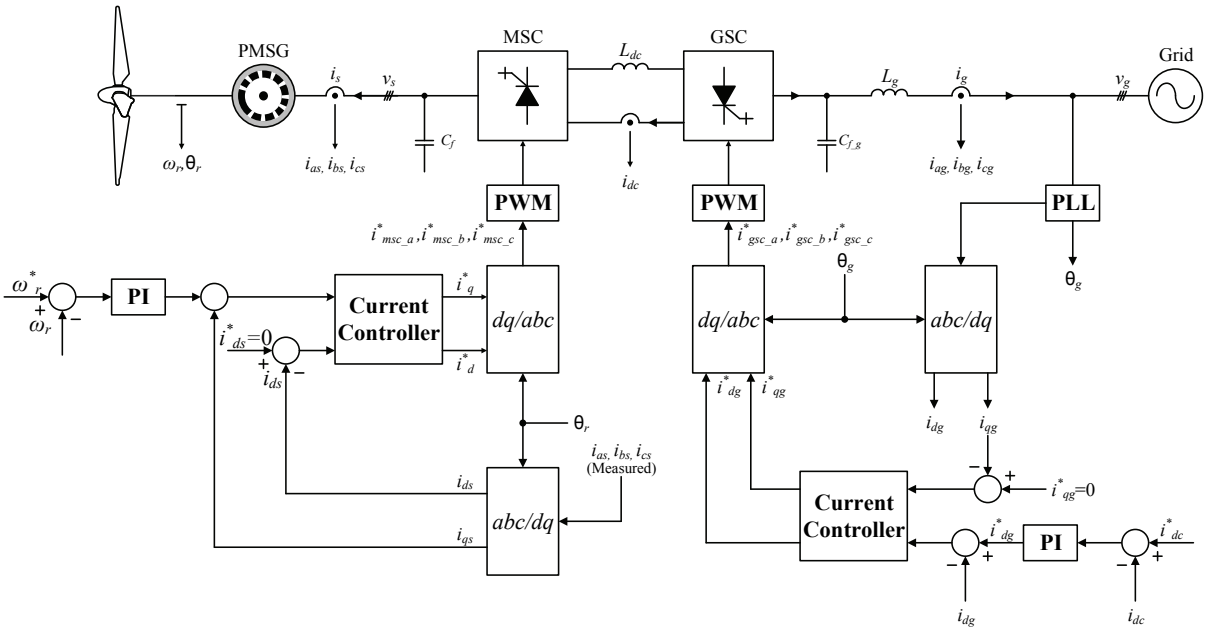

Fig. 9. Overall control block diagram of the two different topologies in Fig. 1 and Fig. 2.

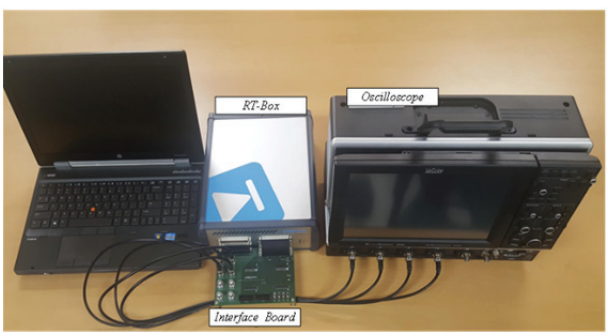

Fig. 10. System configuration of RT-Box.

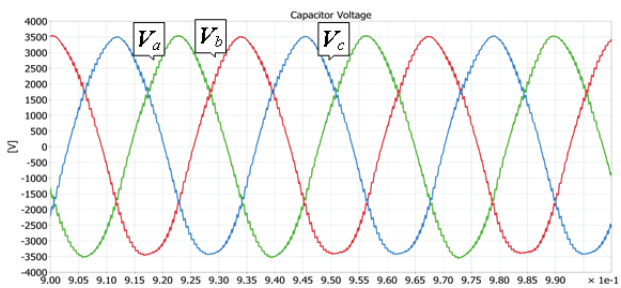

Fig. 11. Simulation waveforms of the current source rectifier capacitor voltage (V_a, V_b, V_c).

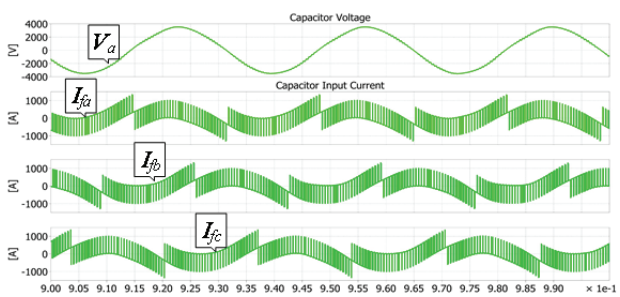

Fig. 12. Simulation waveforms of the current source rectifier capacitor voltage *a*-phase and ripple current (V_a, I_{fa}, I_{fb}, I_{fc}).

TABLE VIII
PERFORMANCE FACTORS OF PMSG SYSTEM UNDER THE RATED POWER CONDITION FROM BOTH OF SIMULATION AND HILS VERIFICATION

Factors	THD of stator current	Electromagnetic torque ripple (peak to peak)
Current Source Rectifier	3.0 %	23 kN.m
Three-phase Three-switch Buck-type Rectifier	3.9 %	31 kN.m

the PMSG and the mechanical torque applied through the prime mover, i.e. the blades of a wind turbine, are illustrated in Fig. 15. The waveforms presented in Figures 11 through 15 are benchmarking targets for the newly proposed three-phase three-switch buck-type rectifier based WTS.

Figures 16 through 20 present simulation waveforms of the three-phase three-switch buck-type rectifier based WTS, particularly for the MSC. These waveforms are measured under the same operating conditions as Table II. The capacitor voltages are described in Fig. 16. In Fig. 17, along with the capacitor voltage of the *a*-phase, the ripple currents of the capacitor filter are also shown. Typical chopped converter input currents of the MSC are described in Fig. 18 along with a filtered sinusoidal waveform of the stator current of the *a*-phase. The stator currents of all three phases and their frequency spectrums are given in Fig. 19. Finally, the electromagnetic torque generated by the PMSG and mechanical

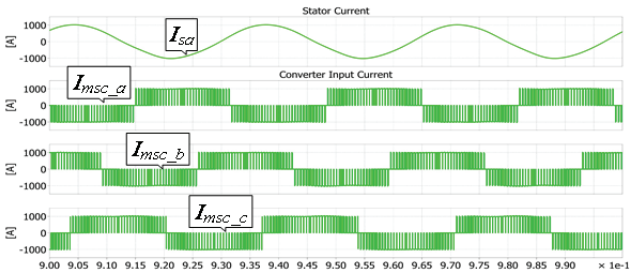

Fig. 13. Simulation waveforms of the current source rectifier stator current *a*-phase and converter input current (I_{sa}, I_{msc_a}, I_{msc_b}, I_{msc_c}).

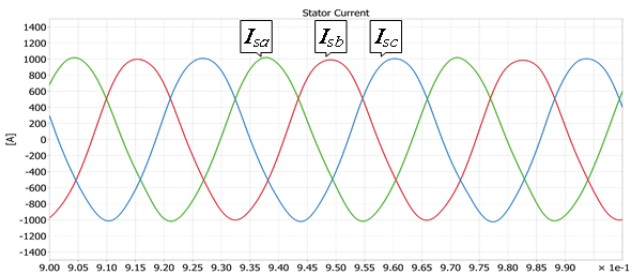

Fig. 14. Simulation waveforms of the current source rectifier stator current (I_{sa}, I_{sb}, I_{sc}).

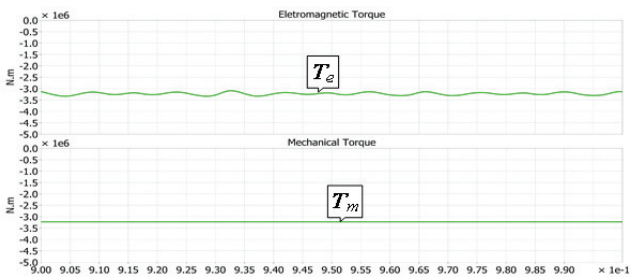

Fig. 15. Simulation waveforms of the current source rectifier electromagnetic and mechanical torque (T_e, T_m).

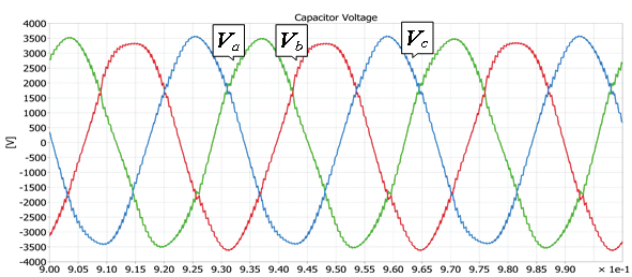

Fig. 16. Simulation waveforms of the three-phase three-switch buck-type rectifier capacitor voltage (V_a, V_b, V_c).

torque applied through the prime mover, i.e. the blades of the wind turbine, are illustrated in Fig. 12. The power factor angle at the converter input node is measured to be 10° leading. In Table VIII, two major performance factors: the Total Harmonic Distortion (THD) of the PMSG stator current and the torque ripple under the rated power condition for the

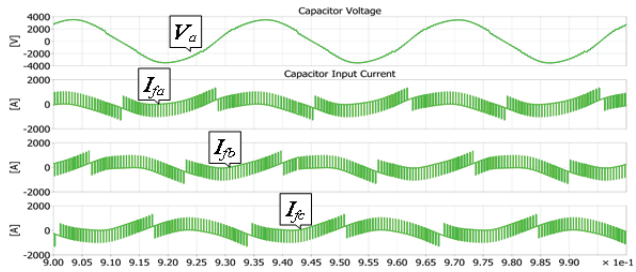

Fig. 17. Simulation waveforms of the three-phase three-switch buck-type rectifier capacitor voltage *a*-phase and ripple current (V_a, I_{fa}, I_{fb}, I_{fc}).

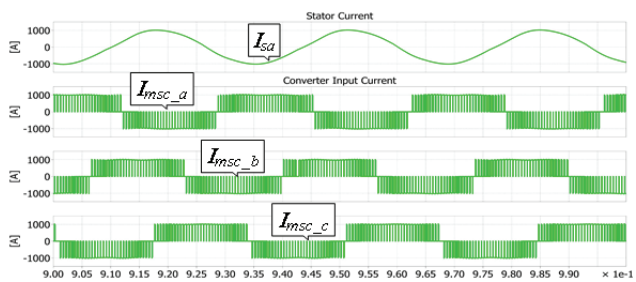

Fig. 18. Simulation waveforms of the three-phase three-switch buck-type rectifier stator current *a*-phase and converter input current (I_{sa}, I_{msc_a}, I_{msc_b}, I_{msc_c}).

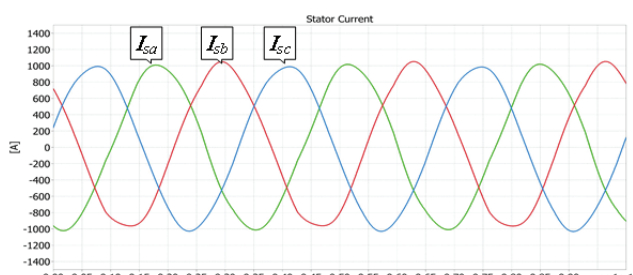

Fig. 19. Simulation waveforms of the three-phase three-switch buck-type rectifier stator current (I_{sa}, I_{sb}, I_{sc}).

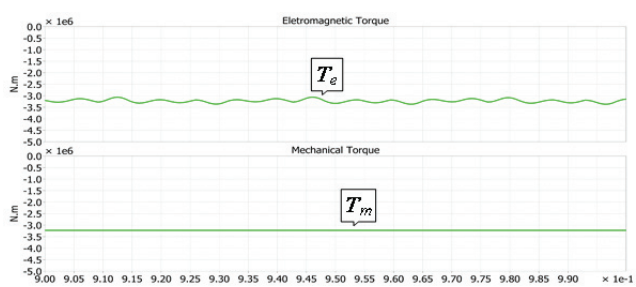

Fig. 20. Simulation waveforms of the three-phase three-switch buck-type rectifier electromagnetic and mechanical torque (T_e, T_m).

two different topologies are obtained and presented. It is noted that even under non-unity power factor conditions, the three-phase three-switch buck-type rectifier based WTS achieves a similar level of performance to that of the current

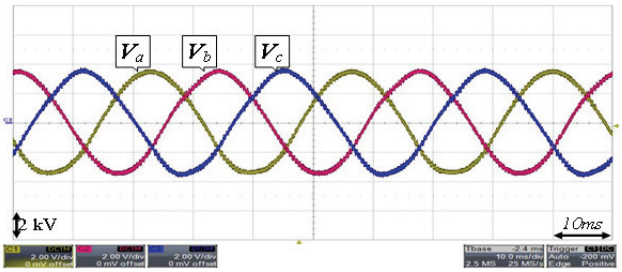

Fig. 21. Experimental waveforms of the capacitor voltage (V_a, V_b, V_c) in the current source rectifier.

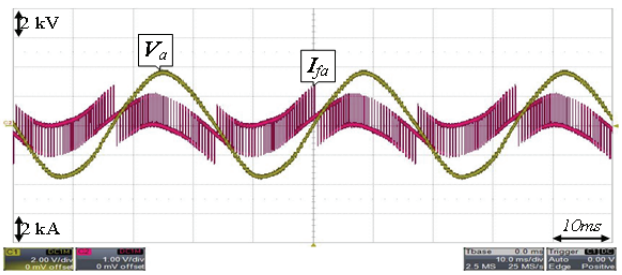

Fig. 22. Experiment waveforms of the current source rectifier *a*-phase capacitor voltage and ripple current (V_a, I_{fa}).

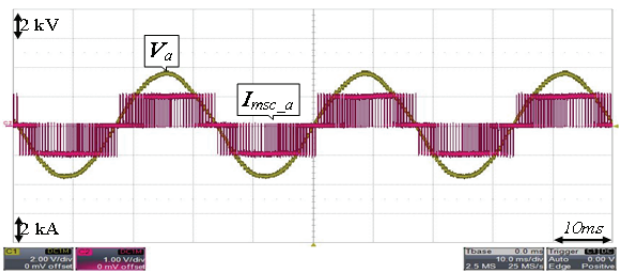

Fig. 23. Experiment waveforms of the current source rectifier *a*-phase stator current and converter input current (I_{sa}, I_{msc_a}).

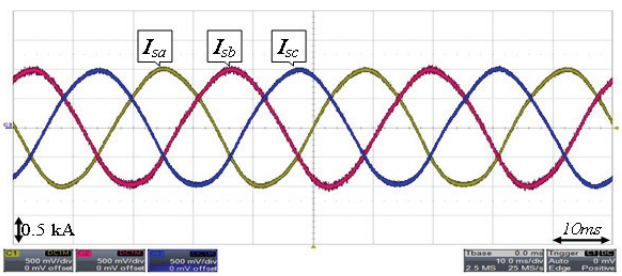

Fig. 24. Experiment waveforms of the current source rectifier stator current (I_{sa}, I_{sb}, I_{sc}).

source rectifier based WTS. It is readily understood that the proposed modulation scheme explained in Table VII is successfully validated.

The parameters of the real-time simulator setup and its operating condition are summarized in Table II. Figure 21 through 25 present experiment waveforms of the current source

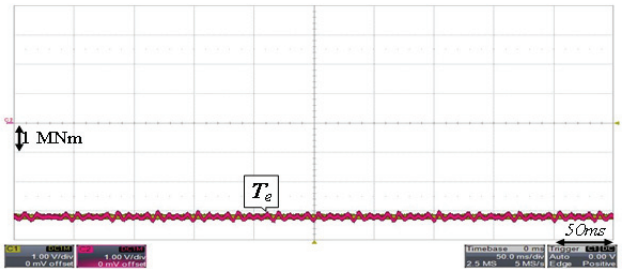

Fig. 25. Experiment waveforms of the current source rectifier electromagnetic torque (T_e).

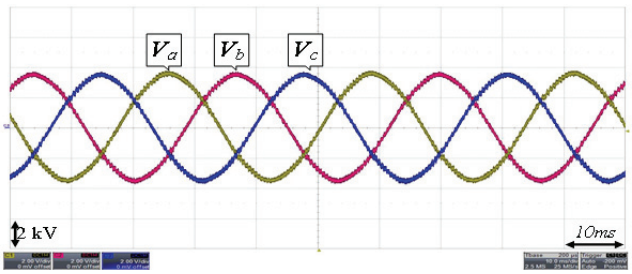

Fig. 26. Experimental waveforms of the capacitor voltage (V_a, V_b, V_c) in the three-phase three-switch buck-type rectifier.

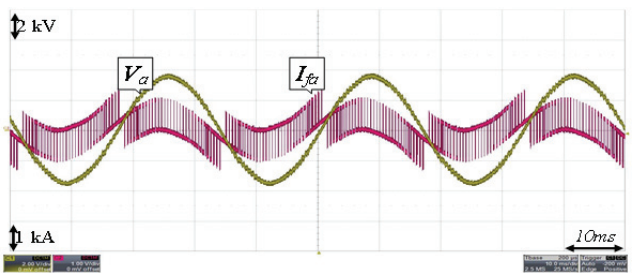

Fig. 27. Experiment waveforms of the three-phase three-switch buck-type rectifier *a*-phase capacitor voltage and ripple current (V_a, I_{fa}).

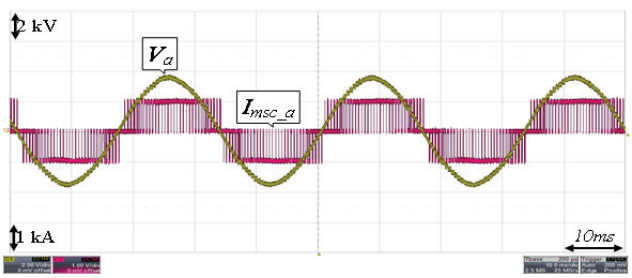

Fig. 28. Experiment waveforms of the three-phase three-switch buck-type rectifier *a*-phase stator current and converter input current (I_{sa}, I_{msc_a}).

rectifier based WTS, particularly for the MSC. These waveforms are measured at the same location as those in Figures 11 through 15. In addition, Figures 26 through 30 show experiment waveforms of the three-phase three-switch buck-type rectifier based WTS, particularly for the MSC.

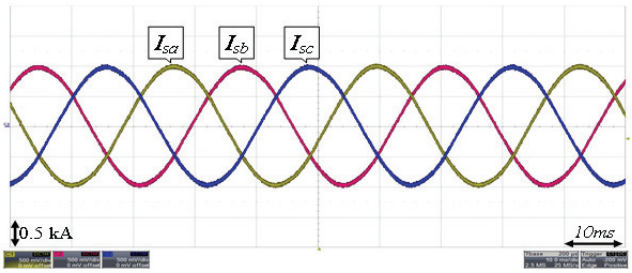

Fig. 29. Experiment waveforms of the three-phase three-switch buck-type rectifier stator current (I_{sa}, I_{sb}, I_{sc}).

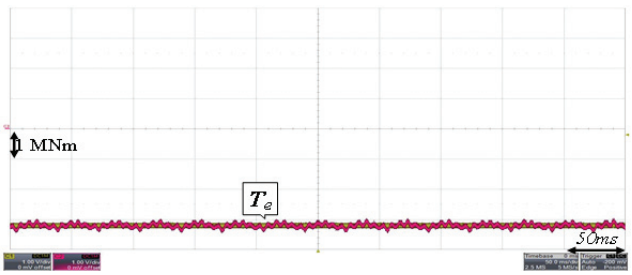

Fig. 30. Experiment waveforms of the three-phase three-switch buck-type rectifier electromagnetic torque (T_e).

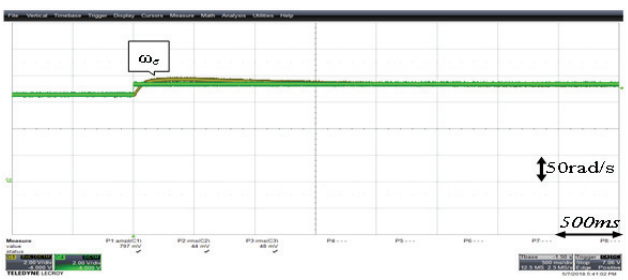

Fig. 31. Experimental waveforms of the PMSG synchronous speed (ω_e) in the current source rectifier.

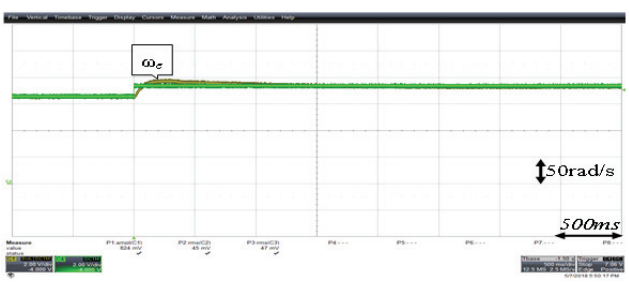

Fig. 32. Experimental waveforms of the PMSG synchronous speed (ω_e) in the three-phase three-switch buck-type rectifier.

These waveforms are also measured at the same location as those of Figures 16 through 20. The experiment waveforms shown in Fig. 21 through 30 exhibit similar characteristics to those of the corresponding simulation waveforms.

To verify the dynamic characteristics of the system, the input wind speed of the PMSG is changed by a step function from 10.5 m/s to 11.8 m/s. The reference value of the synchronous frequency is changed in accordance with the change in the wind speed as a step function. Figures 31 and 32 show that the actual synchronous frequency follows the reference value between the current source rectifier and the three-phase three-switch buck-type rectifier. The reference value of the synchronous frequency is changed from 162.7 rad/s to 182.88 rad/s, and the wind turbine operates at the corresponding speed under the given wind speed conditions.

The actual use of the proposed modulation technique is limited by the operating power factor range. The Diode Rectifier Mode Eliminator can successfully reduce the ripple when the phase difference between the input voltage and the input current of the converter is within the range of -30° to 30°. If the converter operates out of this range, the torque ripple is increased and it may be difficult to achieve stable operation. Therefore, when operating the three-phase three-switch buck-type rectifier based MSC, it is necessary to check the operating power factor of the machine to ensure that it is within the stable operating power factor range.

In the experimental setup of the three-phase three-switch buck-type rectifier, the power factor angle at the converter input node is measured to be 10° leading. In Table VIII, two major performance factors: the Total Harmonic Distortion (THD) of the PMSG stator current and the torque ripple under the rated power condition for the two different topologies are obtained and presented from the experimental results. Simulation and HILS verification results produce THD values of the same amplitude. It is noted that even under non-unity power factor conditions, the three-phase three-switch buck-type based WTS achieves a similar level of performance to that of the current source rectifier based WTS. It is readily understood that the proposed modulation scheme as shown in Table VII is also successfully validated through experiments. As a result, the three-phase three-switch buck-type rectifier can be effectively applied in PMSG wind turbines without suffering from the limited operating range of the power factor in the MSC. The successful utilization of the three-phase three-switch buck-type rectifier as the MSC of PMSG wind turbines can give a rise to many potential engineering approaches to improve the performance of wind turbine. In addition, it can also lower system costs.

VI. Conclusions

This paper proposes a three-phase three-switch buck-type converter as the MSC of wind turbine systems. Owing to a novel switching modulation scheme that eliminates the unwanted diode rectifier mode switching state, the proposed system exhibits satisfying ac voltage and current waveform quality, i.e. THD, up to the level of a typical current source rectifier even under a wide power factor operating range. As shown in this paper, a stator current waveform of high quality

leads to torque ripple characteristics at a similar level tho those of typical current source rectifiers. The presence of a high quality stator current waveform and torque ripple can be regarded as significant advantages for the three-phase three-switch buck-type converter since this topology already has the inherent benefit of a reduced switch count. Therefore, the proposed three-phase three-switch buck-type converter can be considered as a potential candidate for the MSC in wind turbine systems. It can overcome severe design challenges due to relatively tough volume, weight and mechanical vibration limits with respect to the converter placed inside of a nacelle.

ACKNOWLEDGMENT

This research was supported by Korea Electric Power Corporation (Grant number:R18XA04).

REFERENCES

[1] H. J. Lee and S. K. Sul, "Wind power collection and transmission with series connected current source converters," in *Proc. 14th EPE*, pp. 1-10, Aug. 30-Sep. 1, 2011.

[2] J. Sayago, T. Bruckner, and S. Bernet, "How to select the system voltage of MV drives: A comparison of semiconductor expenses," *IEEE Trans. Ind. Electron.*, Vol. 55, No. 9, pp. 3381-3390, Sep. 2008.

[3] K. Lee, K. Jung, Y. Suh, C. Kim, H. Yoo, and S. Park, "Comparison of high power semiconductor devices losses in 5MW PMSG MV wind turbines," *IEEE Applied Power Electronics Conference and Exposition (APEC)*, pp. 2511-2518, Mar. 2014.

[4] O. S. Senturk, L. Helle, S. Munk-Nielsen, and P. Rodriguez, "Power capability investigation based on electro-thermal models of press-pack IGBT three-level NPC and ANPC VSCs for multimegawatt wind turbines," *IEEE Trans. Power Electron.*, Vol. 27, No. 7, pp. 3196-3206, Jul. 2012.

[5] T. Kang, T. Kang, B. Chae, K. LEE, and Y. Suh, "Comparison of efficiency for voltage source and current source based converters in 5MW PMSG wind turbine systems," *Trans. Korean Inst. Power Electron.*, Vol. 20, No. 5, pp. 410-420, Oct. 2015.

[6] J. Dai, D.D. Xu, and B. Wu, "A novel control scheme for current-source-converter-based PMSG wind energy conversion systems," *IEEE Trans. Power Electronics*, Vol. 24, No. 4, pp. 963-972, Apr. 2009.

[7] P. Tenca, A. A. Rockhill, T. A. Lipo, and P. Tricoli, "Current source topology for wind turbines with decreased mains current harmonics, further reducible via functional minimization," *IEEE Trans. Power Electron*., Vol. 23, No. 3, pp. 1143-1155, May 2008.

[8] T. Bruckner, S. Bernet, and P. K. Steimer, "Feedforward loss control of three-level active NPC converter," *IEEE Trans. Ind. Appl.*, Vol. 43, No. 6, pp. 1588-1596, Dec. 2007.

[9] B. Chae, T. Kang, T. Kang, and Y. Suh, "Reduced current distortion of three-phase three-switch buck-type rectifier using carrier based PWM in EV traction battery charging systems," *Trans. Korean Inst. Power Electron.*, Vol. 20, No. 4, pp. 375-387, Aug. 2015.

[10] B. Chae, T. Suh, and T. Kang, "Carrier based PWM for reduced capacitor voltage ripple in three-phase three-switch buck-type rectifier system," *IEEE Energy Conversion Congress and Exposition (ECCE)*, pp. 4609-4616, Oct. 2017.

[11] J. Channegowda, N. A. Azeez, and S. S. Williamson, "Simplified carrier-based modulation scheme for three-phase three-switch rectifier for dc fast charging applications," *IEEE Applied Power Electronics Conference and Exposition (APEC)*, pp. 3504-3506, Mar. 2017

[12] Y. Suh, J. K. Steinke, and P. K. Steimer, "Efficiency comparison of voltage-source and current-source drive systems for medium-voltage applications," *IEEE Trans. Ind. Electron.*, Vol. 54, No. 5, pp. 2521-2531, Oct. 2007.

[13] B. Wu, Y. Lang, N. Zargari, and S. Kouro, "Power conversion and control of wind energy systems," *NJ, IEEE Press*, 2011, ISBN 978-0-470-59365-3.

[14] P. E. Sutherland, "Ensuring stable operation with grid codes," *IAS Magazine*, pp. 60-67, Jan./Feb. 2016.

Beomseok Chae was born in Ulsan, Korea, in 1985. He received his B.S. and M.S. degrees in Electrical Engineering from Chonbuk National University (CBNU), Jeonju, Korea, in 2013 and 2016, respectively. Since 2016, he has been working towards his Ph.D. in Power Electronic Engineering in the Environmental Friendly Energy Conversion Laboratory at Chonbuk National University.

Yongsug Suh (M'90/SM'07) was born in Seoul, Korea. He received his B.S. and M.S. degrees in Electrical Engineering from Yonsei University, Seoul, Korea, in 1991 and 1993, respectively; and his Ph.D. degree in Electrical Engineering from the University of Wisconsin-Madison, Madison, WI, USA, in 2004. From 1993 to 1998, he was an Application Engineer in the Power Semiconductor Division of Samsung Electronics Co., Korea. From 2004 to 2008, he was a Senior Engineer in the Power Electronics & Medium Voltage Drives Division of ABB, Turgi, Switzerland. Since 2008, he has been with the Department of Electrical Engineering, Chonbuk National University, Jeonju, Korea, where he is presently working as a Professor. His current research interests include power conversion systems of high power for renewable energy sources and medium voltage electric drive systems.

Tahyun Kang was born in Gunsan, Korea, in 1982. He received his B.S. and M.S. degrees in Electrical Engineering from Chonbuk National University (CBNU), Jeonju, Korea, in 2013 and 2017, respectively. Since 2017, he has been with the Research and Development Center, Milimsys Co., Seongnam, Korea, where he is presently working as a Researcher.